

TURBULENT CONVECTION AND ANOMALOUS CROSS-FIELD TRANSPORT IN MIRROR PLASMAS

V.P. Pastukhov and N.V. Chudin

Russian Research Centre "Kurchatov Institute", 123182 Moscow, Russia, past@nfi.kiae.ru

Low-frequency quasi-2D plasma convection and the resultant nondiffusive cross-field plasma transport in mirror-based systems are studied by means of direct computer simulations of nonlinear plasma dynamics in a frame of adiabatically reduced one-fluid MHD model. The simulations were performed for axisymmetric or effectively symmetrized paraxial mirror-based systems such as tandem mirror and gas dynamic traps. Various regimes of plasma confinement with sheared plasma rotation were modeled and analyzed. Simulations have shown formation of large-scale flute-like stochastic vortex structures, which are similar to the vortex-like structures observed in GAMMA 10 and GDT experiments. It was shown that a controlled formation of high-vorticity layers allows one to prevent fast plasma degradation and to reduce considerably the nondiffusive cross-field plasma transport even in a presence of unstable pressure driven modes with a weak MHD drive. The effect results from an appreciable nonlinear modification of dominant vortex-like structures due to a competition between pressure driven and Kelvin-Helmholtz instabilities.

I. INTRODUCTION

Anomalous particles and energy transport is one of the crucial problems in magnetic plasma confinement for fusion. Traditionally the majority of plasma researchers associates anomalous transport with plasma fluctuations caused by various drift-wave instabilities^{1,2}. Due to small transverse scales of the drift fluctuations the anomalous transport is conventionally discussed in terms of diffusion approximation with local transport coefficients. However, many recent experiments show that the low-frequency (LF) turbulence and the associated anomalous cross-field plasma transport observed in various magnetic confinement systems with different magnetic field topologies and plasma parameters (tokamaks³⁻⁵, stellarators^{6,7}, tandem mirrors⁸⁻¹¹, etc.) exhibit rather common features, which cannot be appropriately described by a diffusion transport model. In particular, dominant large-scale quasi-2D vortex-like structures with irregular (stochastic) behaviour were revealed in some experiments with magnetized plasma. As a rule, plasma fluctuations in a presence of such stochastic structures

demonstrate frequency and wave-number spectra which are typical for a strong turbulence. Therefore, this phenomenon can be named as "structured turbulence". Stochastic plasma convection caused by the structured turbulence seems to be a reasonable mechanism of nondiffusive cross-field plasma transport.

Large-scale structures those are similar to mentioned above were observed in GAMMA 10 tandem mirrors experiments.^{8,9} These experiments have shown that the plasma rotation with sufficiently high vorticity (high "velocity shear") picked at the axis can appreciably reduce or suppress the large-scale vortex-like plasma convection. The next series of GAMMA 10 experiments^{10,11} have shown that a high-vorticity layer formed and maintained by off-axis electron-cyclotron heating (ECH) can appreciably modify the dominant vortex structures. Soft X-ray tomography and end-loss-analyzer have demonstrated decrease of the observed LF fluctuations and partial decoupling of turbulent structures in the location of the high-vorticity layer. Strong reduction of cross-field thermal flux was also revealed within the layer. This effect looks similar to formation of internal transport barrier (ITB) earlier observed in tokamaks (see review¹²).

Direct computer simulation of self-consistent nonlinear plasma dynamics seems to be an appropriate method for theoretical study of such quasi-2D structured turbulence and the resulting intermittent non-diffusive transport processes. Our previous studies¹³⁻¹⁶ have shown that the simulations based on relatively simple adiabatically reduced one-fluid MHD model demonstrate a rather good qualitative and quantitative agreement with many experiments. Typically the inverse cascade plays an important role in the nonlinear quasi-2D turbulent plasma evolution leading to formation of large-scale dominant vortex-like structures, which are rather independent on space scales of the driving linear instability. In particular, the simulations have shown formation of the large-scale structures in mirror based systems¹⁵. Our simulations were carried out for a simple non-paraxial axisymmetric configuration with divertor stabilization as well as for conditions of traditional paraxial tandem mirrors. Recently, somewhat similar simulations were carried out

by Tsukuba team¹⁷ for a proposed modified GAMMA 10 configuration with non-paraxial divertor at the edge.

Another impressive result for mirror-based systems is drastic improvement of axisymmetric plasma confinement observed in gas dynamic trap (GDT) experiments¹⁸⁻²⁰ with potential biasing applied between ring limiters and grounded end plates. The biasing results in a steep radial jump of plasma potential that forms a layer of sheared plasma rotation. The influence of the potential biasing was demonstrated in regimes without special MHD stabilizers when fast plasma degradation is typically observed due to instability of global $m = 1$ flute-like mode. Both experimental study of fluctuations^{18,20} and computer simulations^{19,20} have shown that the sheared plasma rotation in regimes with the potential biasing considerably modifies the global $m = 1$ mode and transforms plasma confinement to a rather quiet regime, in which large-scale vortex-like structures and the resulting plasma convection are limited radially by the layer of sheared plasma rotation.

Thus, mirror based systems demonstrate a variety of turbulent plasma regimes with nontrivial features. They are very interesting and convenient objects for experimental and theoretical study of many general features of structured turbulence in magnetized plasmas. In this review we briefly present the theoretical basis and the results of self-consistent computer simulations of LF flute-like plasma convection in mirror based systems. The theoretical model is briefly presented in Section II. Section III presents the results of simulations those correspond to experiments at GAMMA 10 and GDT with the potential biasing. Summary is presented in Section IV.

II. THEORETICAL MODEL

The basic theoretical model was developed to study LF nonlinear plasma convection in axisymmetric shearless magnetic systems with closed or open magnetic field lines. An appropriate set of reduced equations²¹ was obtained using method of adiabatic separation of fast (high frequency) and slow (i.e. LF) motions in weakly dissipative one-fluid MHD model. These equations were derived to simulate the LF convection, which is self-consistently generated and maintained by a flute-like pressure driven instability near its threshold in highly non-paraxial systems. The marginally stable plasma state against this mode satisfies the following condition:

$$S = pU^\gamma = \text{const}, \quad (1)$$

where p is plasma pressure and S is a single-valued function of plasma entropy in the specific flux-tube volume $U = dl/B$, γ is adiabatic exponent. Below we assume $\gamma = 5/3$. Under some additional assumptions the equations presented below can be applied to simulate the

flute-like plasma convection in conventional papaxial tandem mirrors as well.

The reduced equations were derived under the assumption that $\beta = 8\pi p/B^2$ is below a critical value for the ballooning Alfvén mode stability threshold and that deviation of plasma pressure profile from the MS state defined by Eq. (1) is small as $\varepsilon^2 \ll 1$ in the presence of the self-consistent turbulent convection. In the weakly dissipative plasmas small parameter ε has the form:

$$\varepsilon \sim (\chi / a c_s)^{1/3},$$

where χ is a background local thermal diffusivity, a is a minor radial scale, c_s is sound speed. In this case, the characteristic frequencies of the nonlinear flute-like convection have to be on the order of $\omega \sim \varepsilon k_\perp c_s$. These convective frequencies are much smaller than the characteristic frequencies of stable magnetosonic ($\omega \sim k_\perp c_A$), incompressible Alfvén ($\omega \sim k_\parallel c_A$), and longitudinal sound ($\omega \sim k_\parallel c_s$) waves. According to Ref.²¹, these assumptions allow us to restrict our further analysis by an adiabatic velocity field \mathbf{v}_a that corresponds to the LF flute-like convection, does not perturb fast stable collective degrees of freedom mentioned above, and describes the relatively slow (adiabatic) plasma dynamics:

$$\mathbf{v}_a = \frac{1}{B^2} [\mathbf{B} \times \nabla \Phi(t, \psi, \varphi)] + \mathbf{B} \lambda \partial_\varphi \Phi(t, \psi, \varphi), \quad (2)$$

where factor λ is determined in Ref.²¹ and describes a longitudinal redistribution of plasma pressure and density in non-uniform magnetic field. It is important that 3D velocity field \mathbf{v}_a is completely described by only one scalar potential function $\Phi(t, \psi, \varphi)$, which is 2D-function in terms of "poloidal" magnetic flux ψ and "toroidal" angle φ (in conventional tokamak terms).

Functional structure of the adiabatic velocity field defined by Eq. (2) prescribes the form of reduced equation of motion. The equation has to be written for a quantity $\hat{w}(t, \psi, \varphi)$ which is a "dynamic vorticity" (i.e. the vorticity of plasma momentum) integrated over the specific magnetic flux-tube volume.²¹ This quantity is the canonic momentum of the reduced adiabatic plasma motion and has the form:

$$\hat{w} = \partial_\psi (\hat{\rho} \langle r^2 \rangle \partial_\psi \Phi) + \partial_\varphi (\hat{\rho} \langle r^{-2} B^{-2} + \lambda^2 B^2 \rangle \partial_\varphi \Phi), \quad (3)$$

where r is the distance from the axis of system symmetry, symbol $\langle \dots \rangle$ denotes averaging over the specific flux-tube volume U , and $\hat{\rho} = \langle \rho \rangle U$ is the mass of plasma in the volume U .

The reduced equation of motion obtained in Ref.²¹ is an exact consequence of initial equation of motion and can be presented in the following form:

$$\begin{aligned}
& \partial_t|_{\psi} \hat{w} + [\Phi, \hat{w}] - \frac{1}{2}[\hat{\rho}, \langle v_a^2 \rangle] \\
& + \partial_{\psi} U \partial_{\varphi} \langle p \rangle = \{DT\}_S, \quad (4) \\
& [\Phi, \hat{w}] \equiv \partial_{\psi} \Phi \partial_{\varphi} \hat{w} - \partial_{\varphi} \Phi \partial_{\psi} \hat{w},
\end{aligned}$$

where symbol $\{DT\}$ on the right-hand side denotes "dissipative terms" those include a local background viscosity (classical or neoclassical) and external sources of momentum. The corresponding reduced equations for S and $\hat{\rho}$ are obtained by integration of initial equations of continuity and heat transfer over the specific flux-tube volume and take the form:

$$\partial_t|_{\psi} \hat{\rho} + [\Phi, \hat{\rho}] = \{DT\}_{\rho}, \quad (5)$$

$$\partial_t|_{\psi} S + [\Phi, S] = \{DT\}_S, \quad (6)$$

where symbols $\{DT\}_{\rho}$ and $\{DT\}_S$ also denote "dissipative terms" those describe the classical (neoclassical) plasma diffusion, thermal conduction, and sources of particles and energy. It is convenient to separate quasi-equilibrium components and fluctuations. We can write functions S and $\hat{\rho}$ as $S = S_0(t, \psi) + \tilde{S}(t, \psi, \varphi)$ and $\hat{\rho} = \rho_0(t, \psi) + \tilde{\rho}(t, \psi, \varphi)$, where S_0 and ρ_0 are the φ -averaged quasi-equilibrium components and $\tilde{S} \sim \varepsilon^2 S_0$ and $\tilde{\rho} \sim \varepsilon^2 \rho_0$ are the fluctuations.

The main force balance is described by Grad-Shafranov equation for the plasma equilibrium. It allows to calculate $\psi(t, r, z)$ using quasi-equilibrium φ -uniform pressure component $p_0(t, \psi) = S_0 / U^\gamma$. φ -averaged part of Eq. (4) determines $w_0(t, \psi)$, i.e. dynamic vorticity of sheared plasma rotation. Knowing this value and using Eq.(3) we calculate radial profile of plasma potential $\Phi_0(t, \psi)$ and frequency $\Omega(t, \psi) = d\Phi_0 / d\psi$ of sheared plasma rotation. φ -averaged parts of Eqs. (5) and (6) describe evolutions of quasi-equilibrium density and entropy components ρ_0 and S_0 (see Ref.²¹ for details). In our previous simulations for mirrors¹⁵ we neglected by density fluctuations and assumed that $\rho_0 \equiv const$. Now we admit nonuniformity of ρ_0 and finite $\tilde{\rho}$. As a result the third term in the left side of Eq. (3) is not equal zero and can provide an additional centrifugal drive for instability. Additionally, we partially account some two-fluid effects such as fixed but arbitrary ratio of ion and electron temperatures T_i/T_e in the background (classical) particle and energy fluxes and thermal force which is proportional to ∇T_e .

Contrary to equations for closed magnetic systems the dissipative terms in the right hand sides of Eqs. (4-6) for mirror-based systems have to account longitudinal losses of momentum, density and energy. Characteristic times of the end losses can be comparable or shorter than the characteristic times of cross-field losses at least for sufficiently quiet regimes with moderate neoclassical cross-field losses and without disruptive MHD events. These losses together with radial distributions of sources can control radial profiles of w_0 , ρ_0 , and S_0 and strongly influence the level of fluctuations. Structure and level of fluctuations as well as the convective cross-field transport can be influenced both by the control of radial profiles and by various line-tying effects.

Reduced equations obtained in Ref.²¹ are formally applicable to axisymmetric magnetic configurations only. However, we apply them also to simulate LF nonlinear flute-like turbulence and the resultant cross-field plasma transport in effectively symmetrized tandem mirror systems such as GAMMA 10. The applicability reasons are the following: axisymmetric central cell gives a dominant contribution to the flux-tube-averaged nonlinear inertial terms 2 and 3 in the left hand side of Eq. (3) (Reynolds stress terms in the equation of motion), which are responsible for nonlinear dynamics and formation of dominant vortex structures; non-axisymmetric anchor cells with anisotropic plasma pressure contribute mainly to linear instability drive and can be effectively accounted as a flux-tube-averaged contribution to the last term in the left hand side of Eq. (3).

Magnetic field configuration of GAMMA 10 and its plasma parameters are presented in Ref.⁸⁻¹¹. Flux-tube-averaged field-line curvature in GAMMA 10 is much less than the inverse length of cross-field plasma pressure gradient, i.e. the magnetic configuration is paraxial one. There is an important distinction in driving forces of linear instability in paraxial tandem mirrors in comparison with the highly non-paraxial case discussed earlier. The gross-rate of linear pressure driven instability is proportional to square root of small effective field-line curvature, which is characterized by small factor $\alpha \propto \partial_{\psi} U$ in the last term of the left hand side of Eq. (3).

Small α in combination with relatively short end-loss times admits an appreciable deviation from the above mentioned marginally stable plasma state. In this case changing particle and energy sources can modify regimes of plasma confinement. In the next section we show that a soft control of w_0 -profile (i.e. control of sheared flow profile) by end-loss term in Eq. (4) can essentially modify the cross-field plasma convection and improve the plasma confinement.

For the tandem-mirror simulations we can use α -factor obtained by means of pressure-weighted flux-tube-averaging. Assuming $\alpha > 0$ we model a weak MHD drive

for nonlinear cross-field plasma convection. We can also try to model a possible trapped particle drive for the convection taking into account that linear trapped particle mode has to be potential one and almost flute-like in the central cell and to decrease only in the anchor cell. Contrary to the ordinary flute-like MHD instability, only modes with sufficiently high azimuthal (toroidal) n -numbers can be linearly unstable due to the trapped particle drive. Therefore, to model the trapped particle drive in system with a weak magnetic well we have to assume that Fourier harmonics of fluctuations with low n -numbers are linearly-stable (i.e. α -factor is negative for them), while harmonics with higher n -numbers are linearly-unstable (i.e. their α -factor is small, but positive).

III. SIMULATION OF FLUTE-LIKE PLASMA CONVECTION IN SYMMETRIZED MIRROR SYSTEMS

Simulations of nonlinear cross-field plasma convection in non-paraxial axisymmetric configurations with divertor stabilization were presented in earlier papers^{15,17}. Fourier harmonic $n = 1$ dominates in the vortex structures at the stage of well-developed nonlinear convection in both simulations. The simulations have shown that a relatively quiet plasma confinement with a moderate cross-field transport can be provided in the axisymmetric systems with divertor stabilization.

In this section we present results of new simulations of self-consistent nonlinear convection in paraxial symmetrized systems. The main attention is paid to an influence of sheared plasma rotation and, first of all, to a competition between fluctuations driven by pressure gradients and fluctuations driven by Kelvin-Helmholtz (KH) instability. The mutual influence of these two drives can prevent fast plasma disruption due to pressure-driven flute-like mode and significantly improve plasma confinement in axisymmetric mirror-based systems without a magnetic well ($\alpha > 0$). To accentuate this effect we reduce an influence of centrifugal drive in the simulations presented below using a flat source of particles that forms low gradient density profiles, while the heating is peaked near the plasma axis and maintains a peaked pressure profile.

Similarly to our previous results¹⁵, regimes with uncontrolled vorticity (uncontrolled potential and rotation profiles) demonstrate formation of monotonically decreasing pressure profiles with a wide negative peak of $w_0(t, x)$ at the axis, where $x = \sqrt{\psi/\psi_{lim}}$ denotes effective dimensionless radial coordinate. In a case of low integral vorticity (weak rotation) simulations show a fast plasma degradation due to a strong $n = 1$ mode both for weak MHD drive ($\alpha > 0$ for all harmonics) and for the "trapped particle" drive. Sufficiently high integral vorticity

suppresses fluctuations in the case of "trapped particle" drive and further enhancement of the integral vorticity can suppress the fluctuations even under the weak MHD drive. This result correlate with results of earlier GAMMA 10 experiments^{8,9}.

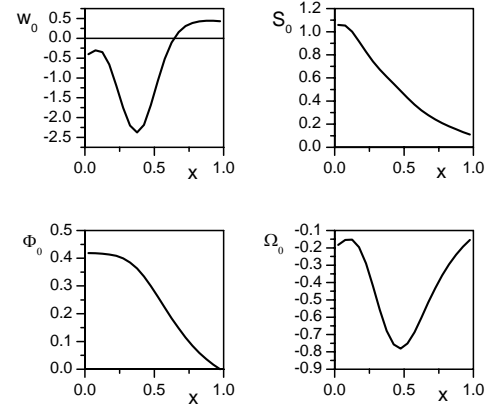


Fig. 1. Profiles of dynamic vorticity w_0 , entropy function S_0 , plasma potential Φ_0 , and plasma rotation frequency Ω in regime (A).

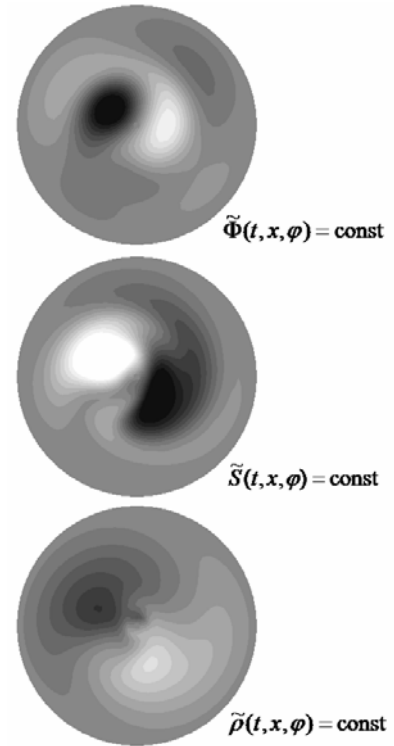


Fig. 2. Typical structures of fluctuations in regime (A).

Regimes with controlled vorticity demonstrate more interesting behaviour. Fig.1 shows parameters of sheared plasma rotation and pressure distribution in regime (A) with the weak MHD drive ($\alpha = 0.001$), in which a

negative peak of dynamic vorticity w_0 is maintained near $x = 0.4$ by an external source of vorticity. These simulations model conditions of GAMMA 10 experiments in which a high vorticity layer was formed and maintained by off-axis ECH^{10,11} near $r \approx 7cm$. In this regime plasma potential Φ_0 is flat or slightly rises near the axis and drops more quickly outside the layer. Fig. 2 illustrates lines of convective flows $\tilde{\Phi}(t, x, \varphi) = \text{const}$ and fluctuations of entropy function (pressure) and density at a stage of well-developed turbulent convection. One can see that the high vorticity layer separate a vortex-like structure of flow-lines with dominant harmonic $n = 1$ in the core area and vortex-like structures with dominant harmonic $n = 2$ at the edge. Large amplitude fluctuations of entropy and density with dominant $n = 1$ are localized in the core area as well. These results correlate with results obtained by end-loss-analyzer and soft X-ray measurements in the GAMMA 10 experiments^{10,11}. Additionally we can compare evolution of chord-integrated plasma pressure (including fluctuations), which are shown at Fig. 3, with experimental soft X-ray tomography presented in Ref. ^{10,11}. Axis x at Fig. 3 corresponds to horizontal axis at Fig. 2. Dimensionless time unit corresponds to $\sim 20ms$ for GAMMA 10.

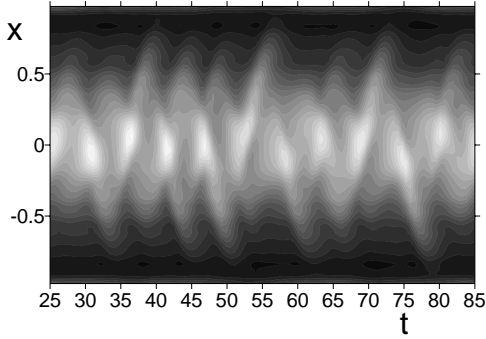


Fig. 3. Evolution of chord-integrated plasma pressure in regime (A) at the stage of well-developed convection.

Fig.4 shows parameters of sheared plasma rotation and pressure distribution in regime (B), which is an attempt to model conditions of GDT experiments¹⁸⁻²⁰ with a positive potential biasing applied between ring limiters and grounded end plates. The total radial potential difference at Fig. 4 approximately corresponds to $700kV$ for GDT parameters. The maximum of $d\Phi_0/dx$ and the corresponding maximum of Ω is maintained near $x = 0.7$ by an external source of vorticity ($x = 0.7$ corresponds to $r \approx 10cm$ for GDT). Without the biasing the plasma shows a fast degradation due to $n = 1$ mode both in experiment and in simulations.

Fig. 5 illustrates flow-lines of well-developed turbulent convection ($\tilde{\Phi}(t, x, \varphi) = \text{const}$) and fluctuations of entropy function and density in regime (B). Like in the regime (A), the vortex-like structures with dominant

harmonics $n = 1$ and $n = 2$ are seen in the core area. But they are less separated from vortex-like structures with dominant harmonics $n = 5$ or $n = 4$ at the edge. More flow-lines cross entire cross-section in the regime (B) in comparison with the regime (A). As a result, the entropy function profile at Fig. 4 is wider than at Fig. 1. Fig. 5 shows that the entropy function fluctuations are also more widely spread in comparison with the regime (A). Fig. 6 illustrates the evolution of chord-integrated plasma pressure in regime (B).

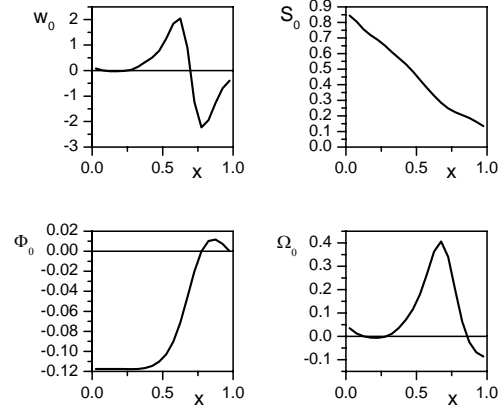


Fig. 4. Profiles of dynamic vorticity w_0 , entropy function S_0 , plasma potential Φ_0 , and plasma rotation frequency Ω in regime (B).

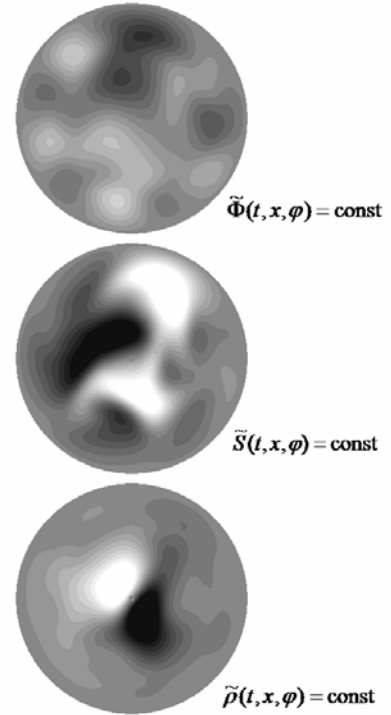


Fig. 5. Typical structures of fluctuations in regime (B).

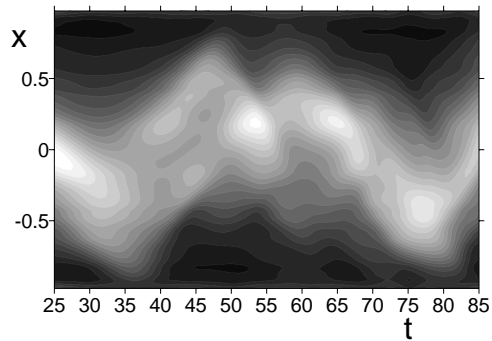


Fig. 6. Evolution of chord-integrated plasma pressure in regime (B) at the stage of well-developed convection.

In additional simulations with $\alpha < 0$ for all harmonics (i.e. without MHD or “trapped particale” drives), the low n -number fluctuations in the plasma core disappear, while fluctuations with higher n -numbers still exist in both examples. Accounting this fact, we can conclude that the core vortex structures were mainly driven by pressure gradient, while the edge vortex structures were maintained by Kelvin-Helmholtz instability generated by sheared plasma rotation. We can also conclude that the main effect of the sheared plasma rotation results from a competition between pressure driven and Kelvin-Helmholtz driven vortex structures.

II. SUMMARY

Simulations of 2D nonlinear flute-like turbulent convection and the resultant cross-field plasma transport were performed for symmetrized mirror-based paraxial systems with controlled and uncontrolled profiles of sheared plasma rotation. The simulations have shown formation of large-scale flute-like stochastic vortex structures, which are similar to those observed in GAMMA 10 and GDT experiments. It was shown that the plasma rotation with the layer of high vorticity can strongly modify nonlinear vortex-like convective structures and prevent the fast plasma degradation even in the case of weak MHD drive. As a rule, the rotation does not stabilize plasma completely, however, the cross-field convective transport is reduced significantly and the plasma confinement becomes a more quiet. The main stabilizing effect of the sheared plasma rotation results from the competition between pressure driven and Kelvin-Helmholtz driven nonlinear vortex-like structures.

ACKNOWLEDGMENTS

We acknowledge Dr. T. Cho for fruitful discussions of experimental results from GAMMA 10. The work was partially supported by State contract 02.740.11.0237 from Russian Federation and by Grant 65382.2010.2 for Support of Leading Scientific Schools in RF.

REFERENCES

1. P.W. TERRY, *Reviews of Modern Physics*, **72**, 109 (2000)
2. P.H. DIAMOND, et al., *Plasma Phys. Control. Fusion*, **47**, R35 (2005).
3. M.R. WADE, and DIII-D Team, *Nucl. Fusion*, **47**, S543 (2007).
4. H. TAKENAGA, and JT-60 Team, *ibid.* **47**, S563 (2007).
5. O. GRUBER, for the ASDEX Upgrade team, *ibid.* **47**, S622 (2007).
6. H. YAMADA, et al., *ibid.* **45**, 1684 (2005).
7. O. MOTOJIMA, et al., *ibid.* **47**, S668 (2007).
8. T. CHO, M. YOSHIDA, J. KOHAGURA, et al., *Phys. Rev. Letters*. **94** 085002-1 (2005).
9. T. CHO, J. KOHAGURA, M. HIRATA, et al., *Nucl. Fusion*. **45** 1650 (2005).
10. T. CHO, J. KOHAGURA, T. NUMAKURA, et al., *Phys. Rev. Letters*, **97**, 055001 (2006).
11. T. CHO, V.P. PASTUKHOV, W. HORTON, et al., *Phys. Plasmas*, **15**, 056120 (2008).
12. R.C. WOLF, *Plasma Phys. Control. Fusion*, **45**, R1 (2003).
13. V.P. PASTUKHOV and N.V. CHUDIN, *Plasma Phys. Reports*, **27**, 907 (2001).
14. V.P. PASTUKHOV and N.V. CHUDIN, *JETP Letters*, **82**, 356 (2005).
15. V.P. PASTUKHOV, and N.V. CHUDIN, *Trans. Fusion Sci.&Tech.*, **51**, 34 (2007).
16. V.P. PASTUKHOV and N.V. CHUDIN, *JETP Letters*, **90**, 651 (2009).
17. I. KATANUMA, et al., *Phys. Plasmas*, **17**, 056120 (2010).
18. P.A. BAGRYANSKY, A.D. BEKLEMISHEV, E.I. SOLDATKINA, *Trans. Fusion Sci.&Tech.*, **51**, 340 (2007).
19. P.A. BAGRYANSKY, A.D. BEKLEMISHEV, M.S. CHASCHIN, E.I. SOLDATKINA (19P45), Radial Electric Fields and Radial Currents in the Gas Dynamic Trap, *Trans. Fusion Sci.&Tech.*, **51**, 337 (2007).
20. A.D. BEKLEMISHEV, P.A. BAGRYANSKY, M.S. CHASCHIN, E.I. SOLDATKINA, *Trans. Fusion Sci.&Tech.*, **57**, 351 (2010).
21. V.P. PASTUKHOV, *Plasma Phys. Reports*, **31**, 577 (2005).